International Journal of Mass Spectrometry 188 (1999) 177–182

Confinement of ions in a radio frequency quadrupole ion trap supplied with a periodic impulsional potential

S.M. Sadat Kiai

Plasma Physics Division AEOI, P.O. Box 11363-8486, Tehran, Iran

Received 24 August 1998; accepted 29 December 1998

Abstract

This article explains the confinement of the ion in the first stability region of the three-dimensional radio frequency quadrupole ion trap using a periodic impulsional potential of the form $V_0 \cos \Omega t/(1 - k \cos 2\Omega t)$ with $0 \leq k < 1$. Numerical computations have been used to study the different aspects of impulsional potential when $k = 0.8$, and compared with a sinusoidal potential $k = 0$ for some value of equivalent points: two operating points located in their corresponding stability diagram having the some β_z. (Int J Mass Spectrom 188 (1999) 177–182) © 1999 Elsevier Science B.V.

Keywords: Confinement; Ions; Quadrupole rf trap; Impulsional potential

1. Introduction

The confinement of ions in rf quadrupole fields in two or three dimensions as in the mass filter or the quadrupole rf ion trap, which is commonly named the QUISTOR (Quadrupole Ion STORage), are well-known processes [1–4]. The utilization of the confined ions in many experiments involving collisions is required to know the initial kinetic energy of the reactants. This situation is particularly so when using a rf ion trap as a dynamic ion–molecule reactions chamber [5–7].

The impulsional voltage given by

$$V(t) = \frac{V_0 \cos \Omega t}{1 - k \cos 2\Omega t} \tag{1}$$

where $\Omega/2\pi$ is the frequency of the rf field and with $0 \leq k < 1$, has an advantage over the classical sinusoidal potential for the ion trap operation. It provides periodic large zero voltage temporal zones where one can inject ions or electrons of well defined initial energy inside the trap for collisional studies, their energy remains unchanged and can be known with accuracy and subsequently adjusted. Fig. 1 shows the Fourier series of voltage 1 involving various k values.

A complete description of the theoretical analyses and its experimental study of periodic impulsional potential 1 is given in [8,9]. It has been found that values of k in the range 0.8–0.9 are a good compromise between an easy simulation of the ion trap and the existence of zero potential zones. The subject of this study is directed to a general survey of the ion trap supplied with potential 1 for various k values, in particular, the comparison between periodic impulsional voltage $k = 0.8$ and the sinusoidal voltage $k = 0$ (classical trap).

PII S1387-3806(99)00019-6

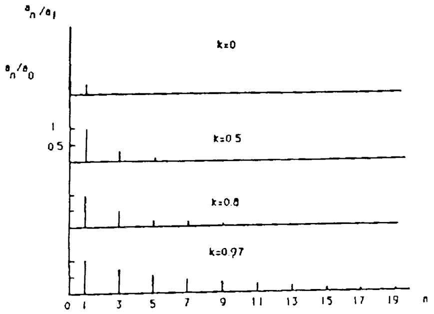

Fig. 1. Fourier series components of the impulsional potential for various values of k.

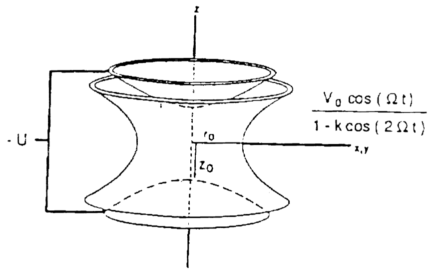

Fig. 2. Electronics configuration.

2. Theory

By using mode III as described by Bonner [10], a negative dc voltage ($-U$) for endcap electrodes and voltage given by Eq. (1) for the ring electrode are shown in Fig. 2. For an ion of mass m and charge e, the basic equation of ion motion is described by Hill's differential equation [11–14] and is given by

$$\frac{\partial^2 u(\xi)}{\partial \xi^2} + \left[a_u - 2I_u \frac{\cos(2\xi)}{1 - k\cos(4\xi)} \right] u(\xi) = 0 \qquad (2)$$

in which u is one of the direction r or z and $2\xi = \Omega t$. The stability parameters a_z and I_z, for the z direction can be written as

$$a_z = \frac{-4eU}{mz_0^2\Omega^2} = -2a_r$$

$$I_z = \frac{2eV_{\max}(1-k)}{mz_0^2\Omega^2} = -2I_r$$

where z_0 is one-half the shortest separation of the endcap electrodes, $r_0^2 = 2z_0^2$ is the square of the ring electrode diameter and $V_0 = (1-k)V_{\max}$. Note when $k = 0$, the ion motions is described by the Mathieu differential equations. However, the stability parameter q_z of Mathieu differs by the factor of $(1-k)$ with respect to I_z of impulsional case, but the stability parameter a_z always stays the same for both sinusoidal and impulsional voltages.

Numerical solution of the Eq. (2) is obtained by employing matrix techniques [15,16]. For the ion motion stability in the fundamental period $\xi = \pi$ and in the absence of space charge density, ion–ion or ion–neutral collisions in the z direction are given by

$$\begin{bmatrix} z(\xi_0+\pi) \\ \dot{z}(\xi_0+\pi) \end{bmatrix} = \begin{bmatrix} \cos(\beta_z\pi) + \alpha_z(\xi_0+\pi)\sin(\beta_z\pi) & \sigma_z(\xi_0+\pi)\sin(\beta_z\pi) \\ -\gamma_z(\xi_0+\pi)\sin(\beta_z\pi) & \cos(\beta_z\pi) - \alpha_z(\xi_0+\pi)\sin(\beta_z\pi) \end{bmatrix} \begin{bmatrix} z(\xi_0) \\ \dot{z}(\xi_0) \end{bmatrix}$$

where ξ_0 represents the initial phase of the rf voltage. The term β_z describes the nature of the ion oscillation

$$\beta_z = \frac{1}{\pi}\arccos\left(\left|\frac{m_{11}+m_{22}}{2}\right|\right)$$

with

$$m_{11} = \cos(\beta_z\pi) + \alpha_z(\xi_0+\pi)\sin(\beta_z\pi)$$

$$m_{22} = \cos(\beta_z\pi) - \alpha_z(\xi_0+\pi)\sin(\beta_z\pi)$$

and the relationship between β_z and the fundamental ion motion (or Secular) frequency ω_z, is given by

$$\beta_z = \frac{2\omega_z}{\Omega}.$$

3. Results

3.1. Stability regions

Fig. 3 shows the first stability regions in the plane (a_z, I_z) for various values of k. In each case the corresponding voltages formed are also presented.

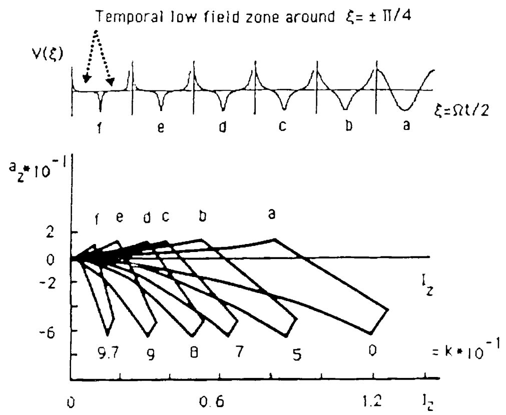

Fig. 3. The first stability diagrams for different k values. In each case the normalized potentials form.

These principal stability diagrams have been found by comparing the trace value of the state transition matrix with the number two, i.e. $|m_{11} + m_{22}| \leq 2$ for a given values of the stability parameters a_z and I_z.

One can note that the a_z values of the apexes of the these stability diagrams do not change, but the values of I_z decrease when k increases. The extreme limits of the parameter I_z versus k and with $a_z = 0$ is shown in Fig. 4.

It is interesting to see how the stability parameters I_z varies with β_z for different values of k. Fig. 5 shows the computed results with β_z in the range of 0–1 and with $a_z = 0$. The linear part of these curves, which follow a simple relationship between $a_z = 0$ and I_z, is called an adiabatic region as in the case of sinusoidal voltage ($k = 0$) the expression $\beta_z = (\sqrt{2}/2)q_z$ has been utilized with the conditions $a_z \approx 0$ and $q_z = I_z \leq 0.4$. For example, the approximated relation in this region for the impulsional voltage ($k = 0.8$) has been found to be $\beta_z = 1.8I_z$.

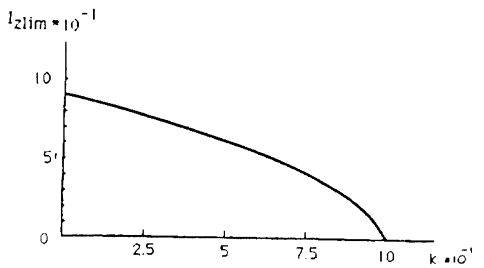

Fig. 4. Extreme limits I_{zlim} of the stability diagrams of the Fig. 3 as a function of k for $a_x = 0$. $k = 0$, 0.1, 0.3, 0.5, 0.7, 0.8, 0.9, 0.97, 0.99, and $I_{\text{zlim}} = 0.909$, 0.9, 0.75, 0.63, 0.46, 0.37, 0.24, 0.12, 0.065, respectively.

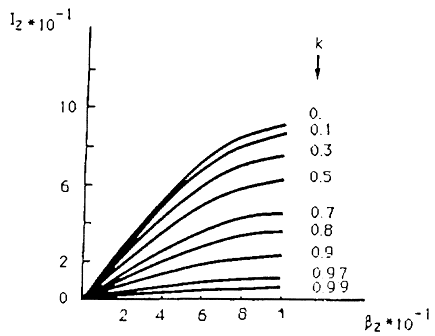

Fig. 5. Stability parameter I_z plotted against β_z for different k values.

3.2. Ion trajectories

For the purposes of comparison of ion trajectories in two different stability diagrams, the equivalent points have been defined as the operating points which have the same value of β_z. Indeed, these points are associated with the same ion oscillation (secular) frequencies ω_z. Fig. 6 shows the computed ω_z frequencies versus k for three equivalent operating points $\beta_z = 0.2$, 0.4, and 0.6 when $a_z = 0$ and $\Omega/2\pi = 1$ MHz.

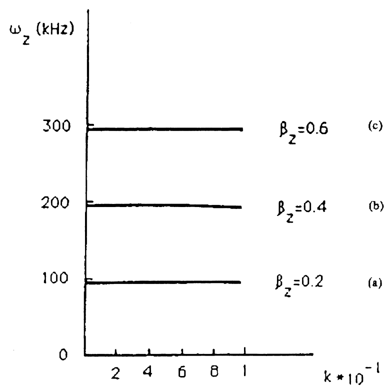

Fig. 6. Variations of secular frequency, ω_z as a function of k, $\Omega/2\pi = 1$ MHz and $a_x = 0$.

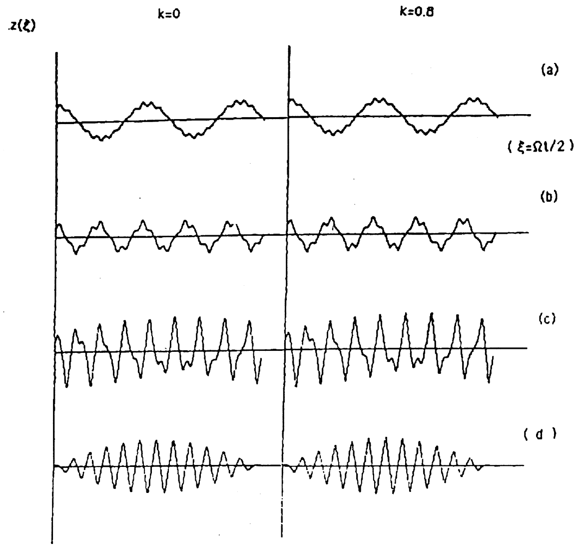

Fig. 7. The ions' displacements as a function of time $\xi = \Omega t/2$ for the same four operating points in two stability diagrams $k = 0$ and $k = 0.8$. The points are as follows: (a) $\beta_z = 0.18$, $k = 0$, $q_z = 0.2539$ and $k = 0.8$, $I_z = 0.1$; (b) $\beta_z \simeq 0.380$, $k = 0$, $q_z = 0.508$ and $k = 0.8$, $I_z = 0.2$; (c) $\beta_z = 0.705$, $k = 0$, $q_z = 0.8$ and $k = 0.8$, $I_z = 0.313$; (d) $\beta_z = 0.959$, $k = 0$, $q_z = 0.906$ and $k = 0.8$, $I_z = 0.355$. The initial phase $\xi_0 = 0$, $z(\xi_0) = 1$, $\hat{z}(\xi_0) = 0$, and 25 fundamental periods ξ.

Ion displacements were examined and displayed both in real time and in the phase space for some characteristic equivalent operating points within two stability diagrams, $k = 0$ and $k = 0.8$. The equivalent points along the I_z axis where $\beta_z = 0.18, 0.38, 0.705$, and 0.959. These points are situated, from left to the right limits of the stability regions and are shown in Fig. 7.

The ion trajectories in the phase space representations are shown in Fig. 8 for two of the ion motions given in Fig. 7. The trajectory points on the $z(\xi)$ and $\dot{z}(\xi)$ coordinates lie on or inside the ellipse, the equation of which depends upon the rf field initial phase ξ_0. The ellipse equation is given by

$$\gamma_z(\xi_0 + \pi) z^2(\xi_0) + 2\alpha_z(\xi_0 + \pi) z(\xi) \dot{z}(\xi_0) + \alpha_z(\xi_0 \pi) \dot{z}^2(\xi_0) = s_z^2$$

where πs_z^2 is the area of the ellipse. The maximum displacement and velocities for a given initial rf field initial phase ξ_0 then can be expressed as

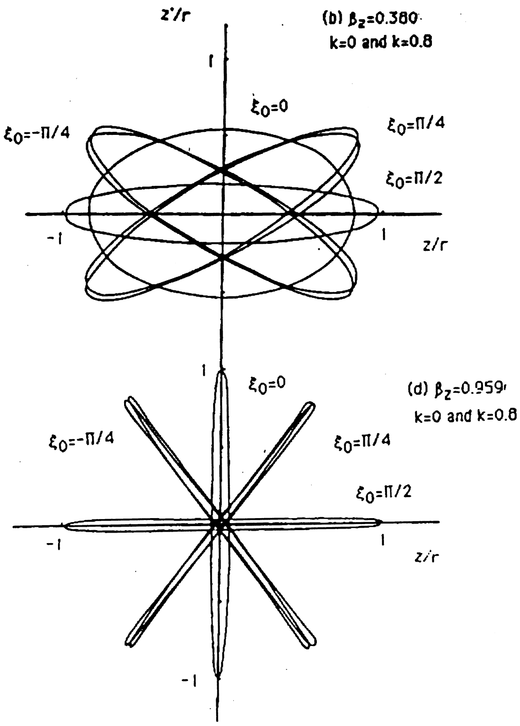

Fig. 8. Family of phase-space ellipses describing motion in the z direction for the same two operating points (b) and (d) as in Fig. 7 and for different phase angle of the drive potential applied to the ring electrode. Note each ellipse has been scaled to $r = (z_{\max}^2 + \dot{z}_{\max}^2)^{1/2}$.

$$Z_{\max}(\xi_0) = s_z[\sigma_{\max}(\xi_0 + \pi)]^{1/2}$$

$$\dot{Z}_{\max}(\xi_0) = s_z[\gamma_{z\,\max}(\xi_0 + \pi)]^{1/2}$$

Fig. 9 shows the evolution of the coefficients γ_z, α_z, and σ_z with ξ_0 for the equivalent operating point $\beta_z = 0.380$ and with $k = 0$, $k = 0.8$ and $a_z = 0$.

3.3. Ion energy

The kinetic energy of the confined ion can be calculated using either pseudopotential well model [17–21], valid only in the adiabatic region of the stability diagrams or phase space dynamic model [22–26] applied in all stability regions. When a pseudopotential well model is considered the equivalent operating points correspond to the same pseudo-

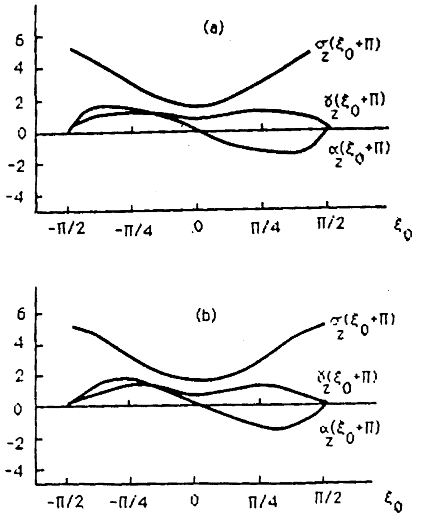

Fig. 9. Variations of $\alpha_z(\xi_0 + \pi)$, $\sigma_z(\xi_0 + \pi)$ and $\gamma_z(\xi_0 + \pi)$ as a function of the initial phase ξ_0 for the same operating point, $\beta_z = 0.380$, (a) $k = 0.8$, (b) $k = 0$.

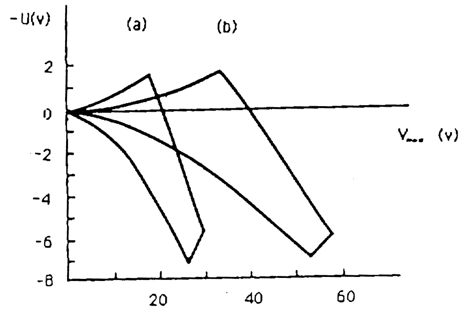

Fig. 10. Comparison of theoretical stability diagrams in the (U, V) space of Xe + ion $\Omega/2 = 1/11$ MHz, $z_0 = 1$ cm. (a) $k = 0.8$, (b) $k = 0$.

potential well depth, according to the following relations:

$$D_z = \frac{eV_{\max}^2}{4mz_0^2\Omega^2}$$

with $k = 0$, or

$$D_z = \frac{(1.8)^2 eV_{\max}^2}{50mz_0^2\Omega^2}$$

with $k = 0.8$. The mean total and maximum kinetic energies of the ion in this case can be written

$$E_T = \frac{8eD_z}{\pi^2}$$

$$E_{\max} = \frac{\pi^2}{4} E_T$$

Taking a typical quadrupole ion trap with $z_0 = 1$ cm, the computed well depth, the total and maximum kinetic energies of the confined Xe^+ ion for the quivalent operating point $\beta_z = 0.233$ are as follows:

$$D_z = 0.925 \quad (\mathrm{V})$$

$$E_T = 0.75 \quad (\mathrm{eV})$$

$$E_{\max} = 1.851 \quad (\mathrm{eV})$$

4. Discussions and conclusions

This computational investigation, using periodic impulsional voltage, having a narrow frequency spectrum for the quadrupole ion trap, suggest that mechanical properties of the confined ions are identical in two different first stability regions, i.e. $k = 0$ and $k = 0.8$, provided that the operating points have the same value of β_z.

The form of periodic impulsional voltage presented in this article merits consideration as it allow existence of zero potential zones of sufficient width for collisional studies, i.e. injection of ions or electrons in the ion trap without a modification of their energies. In addition, this impulsional voltage can substantially reduce the size of the first region of the Mathieu stability diagram. The reduction is in the I_z values as the parameter k is increased from zero, but the stability parameter a_z stays unchanged. The reduction in the (a_z, I_z) space corresponds to an enlargement of the stability region in the $(U, V_{\max})$ plane in Fig. 10.

However, for high values of k, the innate narrow stability region might have special application in the field of mass selections techniques as narrowing of the stability diagram provides rapid transition of stable to unstable ion motion as the stability parameter I_z is varied. More precisely, when the stability region is narrow, higher resolution expected in a short periods of rf impulsional voltage. Investigations are continuing to clarify this last statement.

References

[1] W. Paul, M. Raether, Z. Phys. 140 (1955) S.262.
[2] E. Fisher, Z. Phys. 159 (1959) 26.
[3] H.G. Dehmelt, Adv. At. Mol. Phys. 3 (1967) 53; 5 (1969) 109.
[4] P.H. Dawson, in P.H. Dawson (Ed.), Quadrupole Mass Spectrometry and its Applications, Elsevier, Amsterdam, 1976.
[5] R.F. Bonner, G. Lawson, J.F.J. Todd, R.E. March, Adv. Mass Spectrom. 7 (1974) 377.
[6] G. Lawson, R.F. Bonner, R.E. Mather, J.F.J. Todd, R.E. March, J. Chem. Soc. Faraday Trans. 1 72 (1976) 545.
[7] M. Vedel, These d Etat-Universite de Provence Marseille 20 November 1986.
[8] S.M. Sadat Kiai, J. Andre, Y. Zerega, G. Brincourt, R. Catella, Int. J. Mass Spectrom. Ion Processes 107 (1991) 191.
[9] S.M. Sadat Kiai, Y. Zerega, G. Brincourt, R. Catella, J. Andre, Int. J. Mass Spectrom. Ion Processes 108 (1991) 65.
[10] R.F. Bonner, Int. J. Mass Spectrom. Ion Phys. 23 (1977) 249.
[11] N.W. McLanchlan, Theory and Application of Mathieu Functions, Oxford University Press, London, 1947.
[12] E.T. Whittaker, G.N. Watson, Modern Analysis, Cambridge University Press, Cambridge, 1927, p. 404.
[13] L. Brillouin, Q. Appl. Math. 6 (1948) 167; 7 (1950) 363.
[14] A. Angot, Complements de Mathematiques, 6th ed., Masson and Cie, 1972, p. 219.
[15] L.A. Pipes, J. Appl. Phys. 24 (1953) 902.
[16] M. Baril, Int. J. Mass Spectrom. Ion Phys. 35 (1980) 179.
[17] H.G. Dehmelt, Adv. At. Mol. Phys. 3 (1967) 56.
[18] F.G. Major, H.G. Dehmelt, Phys. Rev. 170 (1968) 91.
[19] J.F.J. Todd, G. Lawson, R.F. Bonner, in P.H. Dawson (Ed.), Quadrupole Mass Spectrometry and its Application, Elsevier, Amsterdam, 1976, p. 181.
[20] G. Lawson, J.F.J. Todd, R.F. Bonner, in D. Price, J.F.J. Todd (Eds.), Dynamic Mass Spectrometry, Heyden, London, 1975, Vol. 4, p. 39.
[21] J.F.J. Todd, R.M. Waldren, R.F. Bonner, Int. J. Mass Spectrom. Ion Phys. 34 (1980) 17.
[22] P.H. Dawson, Int. J. Mass Spectrom. Ion Phys. 20 (1976) 237.
[23] M. Baril, A. Septier, Rev. Phys. Appl. 9 (1974) 525.
[24] P.H. Dawson, Int. J. Mass Spectrom. Ion Phys. 14 (1974) 317.
[25] P.H. Dawson, C. Lambert, Int. J. Mass Spectrom. Ion Phys. 16 (1975) 269.
[26] P.H. Dawson, J. Vac. Sci. Technol. 11 (1974) 269.